ARCHIVES OF ELECTRICAL ENGINEERING VOL. 72(4), pp. 1107–1119 (2023)

DOI 10.24425/aee.2023.147429

Risk of irreversible demagnetisation under transient states of the line start permanent magnet synchronous motor taking into account magnet temperature

TOMASZ ZAWILAK[1] ✉, CEZARY JĘDRYCZKA[2]

[1] *Wrocław University of Science and Technology*
Department of Electrical Machines, Drives and Measurements
Wybrzeże Wyspiańskiego 27, 50-370 Wrocław, Poland
[2] *Poznan University of Technology*
Institute of Electrical Engineering and Electronics
Piotrowo 3A, 60-965 Poznań, Poland
e-mail: ✉tomasz.zawilak@pwr.edu.pl, cezary.jedryczka@put.poznan.pl

(Received: 24.05.2023, revised: 30.09.2023)

Abstract: The paper focusses on the analysis of the demagnetisation process of permanent magnets in line-start synchronous motors in dynamic states related to start-up and resynchronisation. A field-circuit model of electromagnetic phenomena was used to analyse the demagnetisation process, taking into account the influence of temperature on the properties of permanent magnets and their resistance to demagnetisation. The results of the conducted research have shown, among other things, that the process of resynchronisation of the motor is much more dangerous from the standpoint of the risk of demagnetisation than the start-up itself.

Key words: demagnetisation, falling out of step, permanent magnets, synchronous motor

1. Introduction

Permanent magnet synchronous motors with the capability of direct starting through the use of cage rotor windings, i.e. line start permanent magnet synchronous motors (LSPMSMs), have been recently a subject of intensive research [1–3]. Great interest in these machines results from their possibility to obtain higher efficiency and power factor than classical asynchronous machines, with no use of expensive power electronic converter systems. One of the key problems in the research on designing LSPMSMs is to ensure their best possible starting parameters without compromising efficiency and power factor at the steady-state operation. Due to the strong influence of magnetic circuit nonlinearity, field models of electromagnetic phenomena are commonly used in the design of LSPMSM machines [4, 5]. The use of these methods together with advanced optimisation methods allows for the effective design of magnetic circuits for this type of machine [6].

Nevertheless, from the point of view of reliability and fault tolerance, the risk of irreversible demagnetisation of permanent magnets due to transient currents is an important aspect that has not been given much attention so far. The author of reference [7] discussed the complexity of analysing irreversible demagnetisation in LSPMSMs by the use of the FEM. The main concerns involve the need to take into account the influence of temperature on the properties of permanent magnets during the transient states accompanying the start-up process and limited data characterising the permanent magnet immunity to high demagnetising fields. The analysis presented in the paper focusses on the assessment of the risk of irreversible demagnetisation under the second possible transient state of the machine operation, i.e. the resynchronization process that can occur when an LSPMSM is reconnected to the grid after a short-term power outage. The modelling technique that exploits the field circuit model of the resynchronization process has been proposed. Simulations of both start-up and resynchronization processes were carried out, and the results regarding irreversible demagnetisation were compared.

2. Model of the LSPMSM

The presented study of the demagnetisation process was based on the approach proposed by [8]. The field-circuit model of the studied machine was implemented in the professional finite element method (FEM) package Ansys Maxwell (v.2021R2). The planar symmetry of the magnetic field in the studied machine was assumed. To study machine performance and permanent magnet (PM) demagnetisation risk under voltage excitation, the time-stepping algorithm was used to represent time derivatives in the model. The applied field-circuit model consists of two mutually coupled parts: a field part and a circuit part. The model discussed in [8] has been extended by introducing the nonlinear temperature-dependent model of the permanent magnet properties [9]. The structure of the studied machine's cross-section, as well as the view of the applied FE mesh, are shown in Fig. 1.

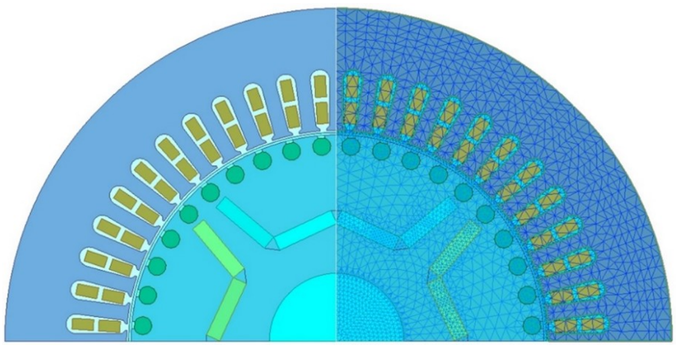

Fig. 1. Geometry and applied FE mesh of the field model of LSPMSM

The rated parameters of the studied machine and the main dimensions of its magnetic circuit are summarised in Table 1.

Table 1. Rated parameters and major dimensions of the motor

Parameter	**Unit**	**Value**
Shaft power	kW	**45**
Speed	rpm	**1500 (4 poles)**
Voltage	V	**400**
Current	A	**68.3**
Power factor	–	**0.98**
Efficiency	–	**0.967**
Stator outer diameter	mm	**368**
Rotor outer diameter	mm	**228**
Core length	mm	**180**
Permanent magnet (PM) material	–	**N42 SH**

3. Model of temperature-dependent permanent magnets demagnetisation

As most demagnetisation curves are highly sensitive to temperature, a temperature increase can cause irreversible demagnetisation. To consider the temperature dependence of the demagnetisation behaviour, the approach discussed in detail in [10] has been adopted. Since temperature-dependent parameters of the magnet are typically described in supplier datasheets by means of the intrinsic flux density B_i versus the magnetic field strength H curve, it is advantageous to formulate the model by taking into account that:

$$B = B_i + \mu_0 H. \tag{1}$$

The temperature T dependence of B_i and coercivity can be adequately described by the hyperbolic tangent function with two terms such as [10]

$$B_i(H,T) = P(T)\left(b_0 \tanh\left(\frac{H + Q(T)H_{ci}(T_0)}{Q(T)h_0}\right) + b_1 \tanh\left(\frac{H + Q(T)H_{ci}(T_0)}{Q(T)h_1}\right)\right), \tag{2}$$

where μ_0 is the magnetic permeability of the air coefficients b_0, b_1, h_0, h_1 can be determined based on the input of the B_i–H curve at the reference temperature T_0.

The magnetic permeability of the recoil line at the given temperature can be derived from (1) and (2) as

$$\mu(T) = \left.\frac{\partial B_i(H,T)}{\partial H}\right|_{H=0} + \mu_0 = \frac{P(T)}{Q(T)}\mu_i(T_0) + \mu_0\,. \tag{3}$$

There

$$P(T) = \left(1 + \alpha_1 (T - T_0) + \alpha_2 (T - T_0)^2\right), \tag{4}$$

$$Q(T) = \left(1 + \beta_1 (T - T_0) + \beta_2 (T - T_0)^2\right), \tag{5}$$

where α_1, α_2 as well as β_1 and β_2 are coefficients that are provided in supplier datasheets.

4. Validation of the model of nonlinear permanent magnet

Magnetic properties of magnetically hard materials strongly depend on temperature. In general, the increase in temperature deteriorates the remanent magnetic flux density as well as coercive force. Until recently, in computer simulations applying field methods, the widely used today permanent magnets based on rare earth components have been treated as linear materials [6, 11]. In order to account for the effect of permanent magnet temperature on the performance of designed electromechanical transducers, in the design calculations, the calculations assumed that the temperature of the magnets was known in advance and accounted for its effect by a linear change in the magnet remanent magnetic flux density defined by the coefficient k_B. The influence of temperature on permanent magnets is more complex, especially when the demagnetisation process needs to be studied. For such an analysis, the nonlinearity of the *BH* curve with respect to magnetic field intensity as well as temperature must be taken into account. The temperature influence is typically described by the set or family of *BH* curve characteristics at different temperatures, see the example of *BH* curves for the applied permanent magnet material shown in Fig. 2.

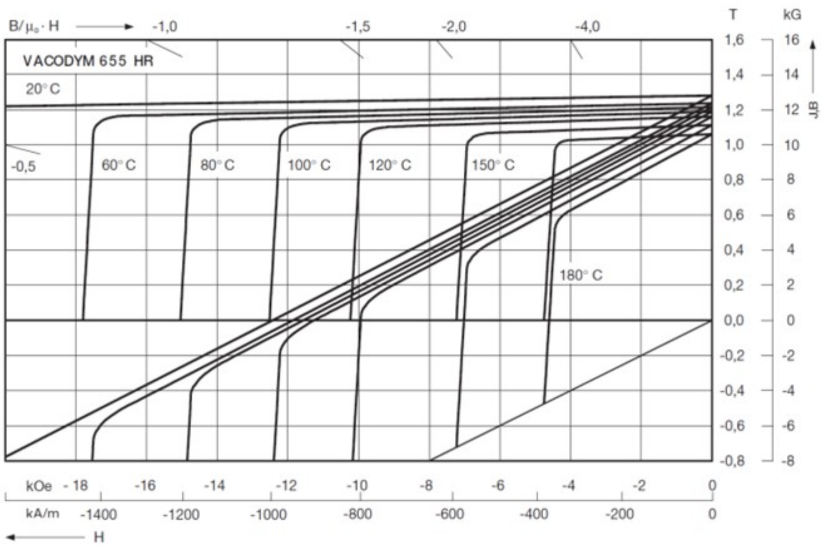

Fig. 2. Demagnetisation curves of the N42SH permanent magnets

Based on the characteristics presented above and the design of the magnetic circuit of the studied motor (air-gap length of 2.5 mm) it can be expected that for temperatures above about 160 Celsius degrees, the magnetic voltage drop in the air-gap of the machine should lead to the demagnetisation process. To validate the model, simulations of open-circuit operation of the motor at rated speed were carried out to determine the influence of the permanent magnet temperature on the electromotive force (*emf*). In the simulations, the magnet temperature has been defined as a parameter known in advance, and the calculations have been repeated for a temperature in the range of 20 to 230 Celsius degrees with a step of 5°C. The determined *rms* value of the phase back-*emf* as a function of magnet temperature has been shown in Fig. 3.

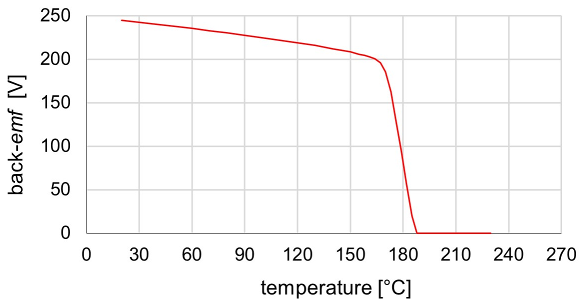

Fig. 3. Open-circuit back-*emf* at rated speed as a function of magnet temperature

The obtained results allow one to state that the applied model of the permanent magnet meets theoretical expectations. Nevertheless, it should be emphasised that experimental verification of the model is very difficult because such tests destroy the machine. The outcomes are also in line with findings reported by [7], where experimental validation of a nonlinear model of the magnet has been carried out; however, in limited temperature ranges to avoid irreversible demagnetisation.

5. Steady state asynchronous characteristics

When designing the magnetic circuit of the LSPMSM, one of the main objectives is to strive for the best possible starting properties, in particular high starting torque and low inrush current during start-up, without deterioration of steady-state synchronous performance regarding efficiency and power factor. In classical induction motors, high starting torque and reduced inrush current are achieved by increasing the cage resistance. A higher resistance of the cage winding shifts the breakdown slip towards lower rotor speeds and consequently increases the starting torque [12, 13]. In the classical asynchronous machines, the drawback of high resistance of the cage winding is, of course, that the motor efficiency deteriorates as due to increased rotor losses. In case of LSPMSMs, since the cage winding resistance after synchronisation in a steady state has no direct impact on the motor efficiency, the increase of cage winding resistance allows one to reduce the inrush current and increase the start-up torque. However, as a consequence of the higher breakdown slip value, the pull-in synchronism torque also decreases, which may lead to the failure of motor synchronization at high inertia loads [5]. Squirrel cage windings with increased resistance are also used in LSPMSMs with a switchable number of pole pairs, in which the synchronisation process is performed in the so-called top-down manner, i.e. from speeds higher than synchronous for rated operating conditions. It should be noted that the manipulation of the rotor winding resistance not only influences the starting characteristics of the machine but also has a significant impact on the resistance of permanent magnets to demagnetisation.

During the design process, the resistance of the cage winding can be influenced either by changing the shape and cross-section of the rotor slots or directly by the conductivity σ of the cage conductor material. In the presented approach, in order to evaluate the impact of cage resistance on starting torque, locked rotor current, as well as the demagnetisation process, the change in the cage resistance has been achieved by assuming a different value of cage winding conductivity. Such an approach allowed us to fix the geometry of the rotor and thus not to introduce any additional factors in the analysis like change of the saturation level, etc.

One of the approaches to assess the starting properties of the LSPMSM is to investigate the torque and current values determined for fixed rotor speeds at the asynchronous operation range. The torque and current values are determined using the developed field model as average and *rms* values, respectively, for one period supply voltage after reaching the electromagnetic steady state operation. The steady-state torque and current vs. speed characteristics were examined for the studied machine assuming different conductivity σ of the cage winding material: a) σ = 48 MS/m, b) σ = 24 MS/m, c) σ = 12 MS/m and d) σ = 6 MS/m speed characteristics.

The determined steady-state torque and current vs. speed characteristics have been presented in Fig. 4(a) and 4(b), respectively.

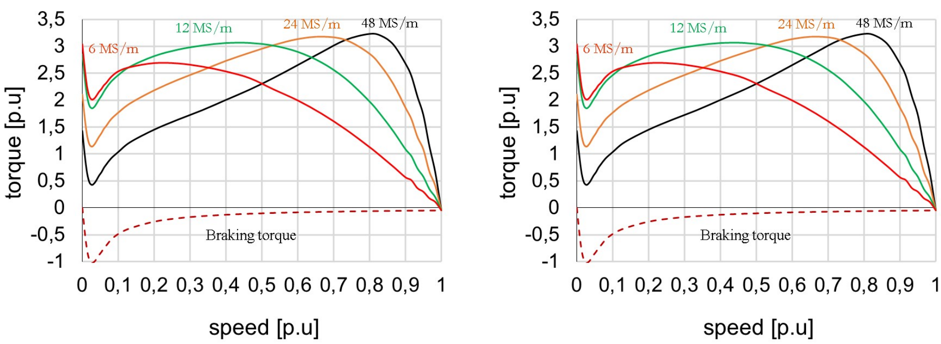

(a) (b)

Fig. 4. Characteristics of: steady state of electromagnetic torque (a) and current (b) for selected materials of the rotor cage winding

Analysing the determined characteristics, it can be noted that the results confirm the predicted impact of the cage resistance, i.e. that an increase in cage winding material conductivity leads to a decrease in the value of the breakdown slip. Moreover, due to the influence of the braking torque produced by the magnets, the decrease in the breakdown torque can be observed for a cage material of σ = 12 MS/m (c) and σ = 6 MS/m (d).

Focussing on the steady-state current at zero speed, it can be seen that, as expected, increasing the cage winding resistance allows one to reduce the effective current of the motor during its start-up. What is more important the decrease of cage winding conductivity results in increase of the start-up torque.

6. Demagnetisation process at transient states

A comparative analysis of transient states in the LSPMSM has been performed in order to evaluate the risk of permanent magnet partial demagnetisation. As discussed in the introduction section, three main transient state conditions of LSPMSM operation can be distinguished [14–16]: a) start-up process, i.e. sate occurring under synchronization when the rotor speed increases from zero to the speed close to the synchronous speed driven by the asynchronous torque and then is pulled into synchronism by superposition of asynchronous torque and pull into synchronism torque as a result of magnetic flux exited by the rotor magnets, b) resynchronization process, which is a transient state that can occur as a result of a short-term power outage, in this state the motor is reconnected to the grid when its rotor speed is close to synchronous speed, and c) when the motor is synchronised with a speed higher than the synchronous speed, i.e. when the motor has pole-changing winding [17] or is equipped with an additional starting winding having a lower number of pole pairs than the main steady-state operation winding. In the proposed paper, only two of the abovementioned transient states are studied, i.e. cases a) and b). It should be noted that from the perspective of electromagnetic phenomena, the over-synchronisation (i.e. synchronisation at a rotor speed slightly higher than the synchronous speed) is quite similar to a resynchronisation process.

First, the resynchronisation process was analysed, the torque and current waveforms were determined assuming different values of the initial electrical angle δ_i. This angle can be treated as a parameter that represents the "electrical" position of the rotor at the time of the reconnection of the machine to the grid. δ_i is equal to 0 deg when the phase of the induced *emf* in a given phase winding is equal to the phase of the corresponding supply phase voltage. When δ_i is equal to 180 deg, it means that the reconnection occurred when the induced voltage was in counter-phase with the corresponding supply voltage. The obtained torque and current waveforms have been shown in Figs. 5 and 6, respectively.

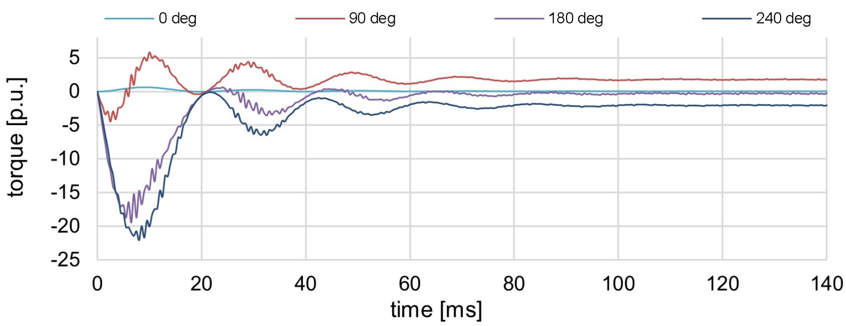

Fig. 5. Electromagnetic torque waveforms during motor resynchronization for different values of initial δ_i angle

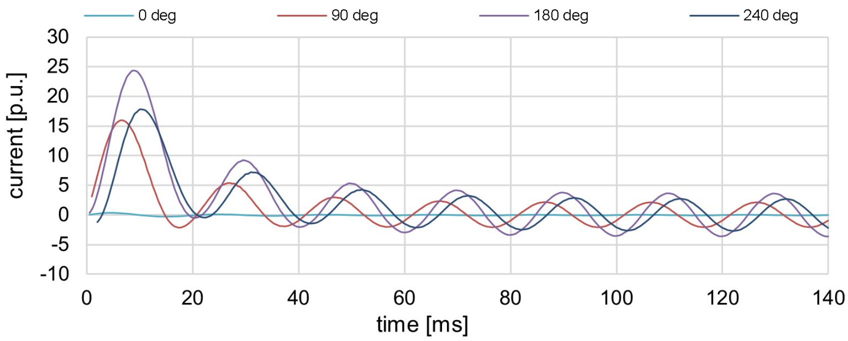

Fig. 6. Phase current waveforms during motor resynchronization for different values of initial δ_i angle

In the second stage, the start-up process was analysed, the torque and current waveforms were determined assuming different values of the initial electrical angle δ_i. The determined torque and current waveforms have been shown in Figs. 7 and 8, respectively.

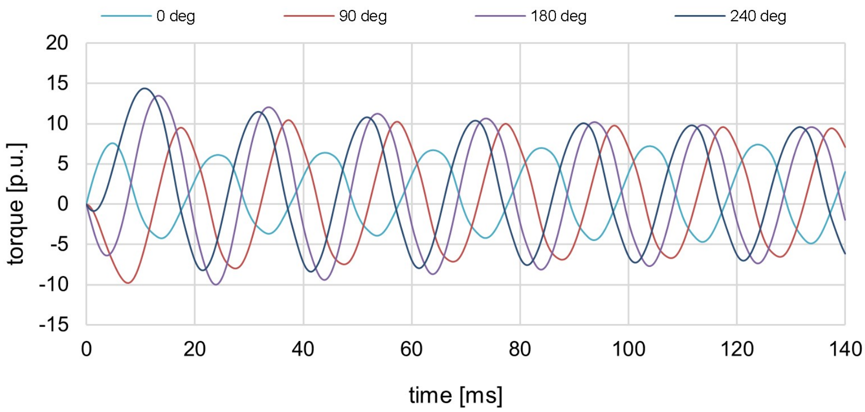

Fig. 7. Electromagnetic torque waveforms during motor start-up for different values of initial δ_i angle

As can be noted from the above results, the resynchronization process for δ_i seems to occur around 180 deg, which is more dangerous in terms of the risk of partial demagnetisation than the transient process related to starting the machine. In order to confirm this finding, the drop of the back-*emf* value after the transient state has been analysed. The linking procedure of the permanent magnet magnetization state has been applied. The simulations have been carried out for different values of δ_i, and to investigate the impact of cage winding resistance on the conductivities of cage winding materials studied in section IV. The simulations assumed a permanent magnet

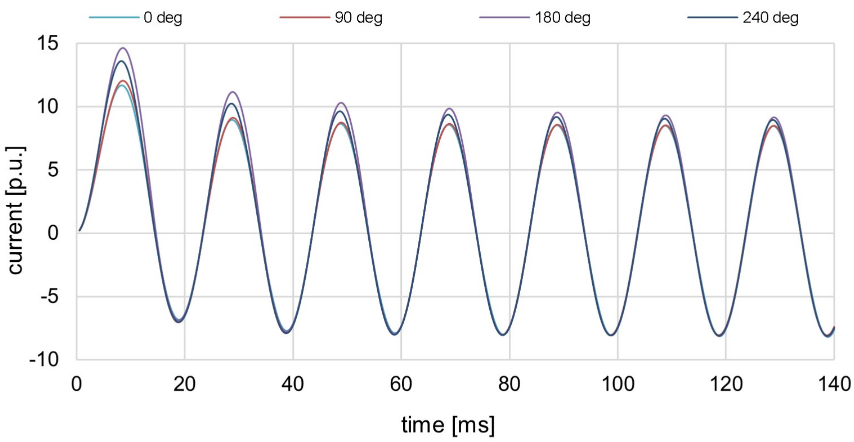

Fig. 8. Phase current waveforms during motor start-up for different values of initial δ_i angle

temperature of 80 degrees Celsius. The determined characteristics of phase back-*emf* values as a function of δ_i for the studied resynchronization and start-up process have been shown in Fig. 9(a) and 9(b), respectively.

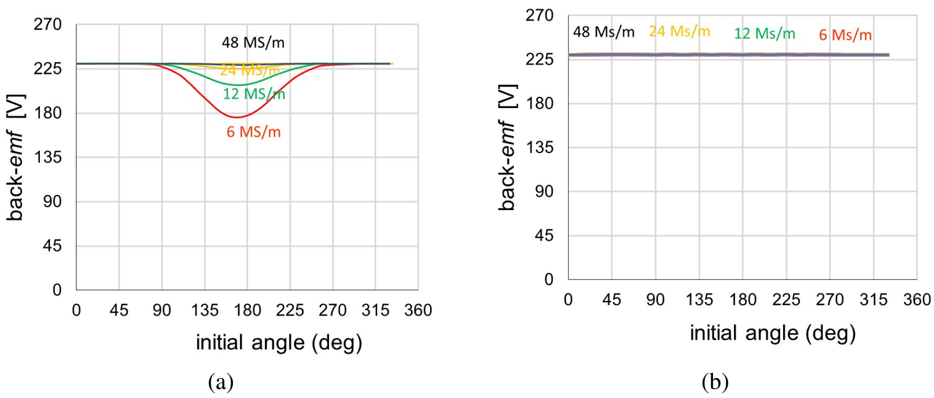

Fig. 9. Induced voltage in the no-current state after the transient state as a function of the initial angle for different cage conductivities resynchronization (a); start-up (b) (magnet temperature 80°C)

The comparison of the obtained characteristics based on the conducted research confirms that the resynchronization process can be much more dangerous in terms of the risk of irreversible partial demagnetisation than the start-up process. The irreversible decrease in the back-*emf* value is especially apparent for a low conductivity of the cage material at the initial angle δ_i close to but slightly less than 180 deg – detailed analysis shows that the worst conditions for the studied machine appear for δ_i equal to about 170 deg.

In the next stage, the influence of magnet temperature on the partial demagnetisation process at resynchronization and start-up processes has been examined. The conducted research assumed the "worst-case scenario" conditions in terms of the initial angle δ_i. For the simulations of the resynchronization process, the assumed value of δ_i was equal to 170 deg, while for the start-up process, δ_i was equal to 0 deg. The influence of the magnet temperature on the back-*emf* value after considered transient states has been illustrated in Fig. 10(a) and Fig. 10(b) for resynchronization and start-up processes, respectively.

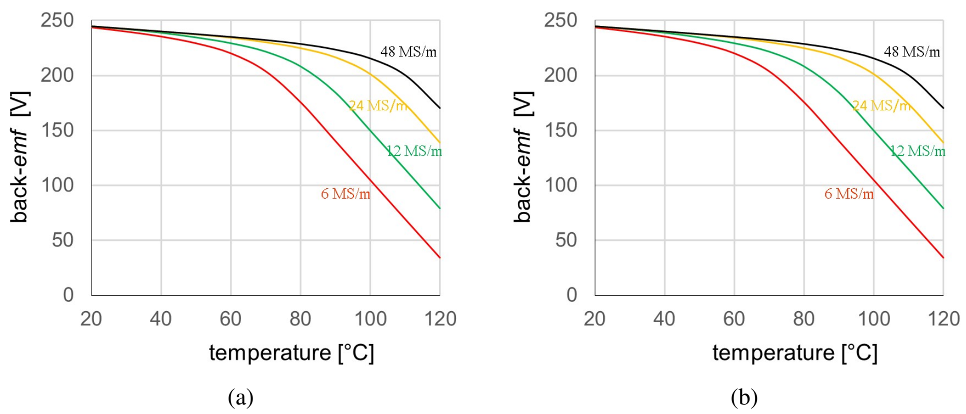

Fig. 10. Induced voltage at the no-current condition as a function of magnet temperature after transient state under the worst case conditions: resynchronization (a) and start-up process (b)

As can be observed on the magnet temperature graph, the cage winding resistance has a significant impact on the irreversible partial demagnetisation of the magnets. It should be emphasised that the deterioration of the back-*emf* is much stronger after resynchronization than after the machine start-up process. It should also be noted that for the studied machine for the cage conductor material of low conductivities (6 and 12 MS/m) the irreversible demagnetisation occurs even at low temperatures of the magnet (about 60 to 80°C). It should also be noted that the irreversible demagnetisation of the poor-conductivity cage conductor material (6 and 12 MS/m) in the tested machine occurs even at low magnet temperatures (approximately 60 to 80°C). It should be kept in mind that the resynchronization process is more likely to occur at high temperatures of the magnets than the start-up process.

In order to protect the machine against the risk of demagnetisation at the design stage of the LSPMSM, an analysis of the demagnetisation process should be carried out together with an analysis of the impact of cage winding resistance.

The next test of the studied machine investigated the influence of cage winding material conductivity on the degree of demagnetisation at assumed magnet temperatures. As can be seen from the determined characteristic of the back-*emf* as a function of cage material shown in Fig. 11, even at a temperature of 80°C the machine can be damaged when reconnected to the grid under of the 'worst case scenario' conditions.

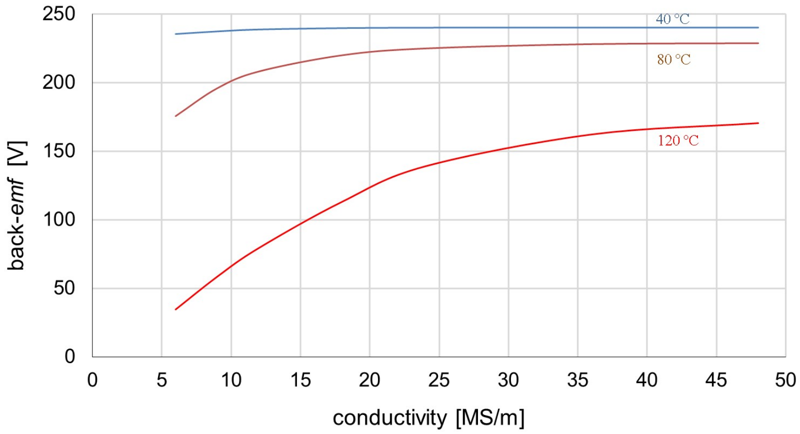

Fig. 11. Induced voltage as a function of the conductivity of the cage winding after resynchronization under the most unfavourable conditions (δ_i = 70 deg)

7. Conclusion

The paper analyses the demagnetisation process of permanent magnets in LSPMSMs. The field-circuit model of electromagnetic phenomena in the machine has been implemented in the Ansys Maxwell professional FEM package and employed in the conducted research. The proposed approach studies the nonlinear magnetic properties of the permanent magnet, considering the influence of temperature.

To determine the most unfavourable conditions that occur during the transient state operation of the LSPMSM, which can lead to irreversible deterioration of permanent magnet properties and, in consequence, damage the machine, a number of simulations were carried out using a developed model of the LSPMSM. On the basis of the conducted research, it was shown that the highest risk of demagnetisation occurs during resynchronization of the motor, when the induced electromotive forces are almost in counter-phase (170 deg) to the supply voltage waveforms.

The conducted comparative analysis between the impact of the transient inrush armature reaction field at the start-up and the resynchronization processes showed that the resynchronization process during machine operation is much more dangerous in terms of irreversible demagnetisation of the magnets than the machine starting itself.

The carried out investigations showed that apart from temperature, one of the crucial factors significantly affecting the demagnetisation process is the resistance of the rotor cage winding. It has been shown that an increase in the value of the cage winding resistance leads to a weakening of its shielding action, which can cause permanent motor damage.

Based on the conducted research, it was concluded that to protect the machine against the risk of demagnetisation, an analysis of the demagnetisation process should be carried out at its design stage, together with an analysis of the impact of cage winding resistance taking into account magnet temperature.

References

[1] De Almeida A.T., Ferreira F.J.T.E., Duarte A.Q., *Technical and Economical Considerations on Super High-Efficiency Three-Phase Motors*, IEEE Transactions on Industry Applications, vol. 50, no. 2, pp. 1274–1285 (2014), DOI: 10.1109/TIA.2013.2272548.

[2] Hassanpour Isfahani A., Vaez-Zadeh S., *Line start permanent magnet synchronous motors: Challenges and opportunities*, Energy, vol. 34, no. 11, pp. 1755–1763 (2009), DOI: 10.1016/j.energy.2009.04.022.

[3] Palangar M.F., Soong W.L., Bianchi N., Wang R.-J., *Design and Optimization Techniques in Performance Improvement of Line-Start Permanent Magnet Synchronous Motors: A Review*, IEEE Transactions on Magnetics, vol. 57, no. 9, pp. 1–14 (2021), DOI: 10.1109/TMAG.2021.3098392.

[4] Jedryczka C., Wojciechowski R.M., Demenko A., *Finite element analysis of the asynchronous torque in LSPMSM with non-symmetrical squirrel cage winding*, International Journal of Applied Electromagnetics and Mechanics, vol. 46, no. 2, pp. 367–373 (2014), DOI: 10.3233/JAE-141947.

[5] Baranski M., Szelag W., Lyskawinski W., *An analysis of a start-up process in LSPMSMs with aluminum and copper rotor bars considering the coupling of electromagnetic and thermal phenomena*, Archives of Electrical Engineering, pp. 933–946 (2019), DOI: 10.24425/aee.2019.130693.

[6] Jędryczka C., Knypiński Ł., Demenko A., Sykulski J.K., *Methodology for Cage Shape Optimization of a Permanent Magnet Synchronous Motor Under Line Start Conditions*, IEEE Transactions on Magnetics, vol. 54, no. 3, pp. 1–4 (2018), DOI: 10.1109/TMAG.2017.2764680.

[7] Baranski M., Szelag W., Lyskawinski W., *Experimental and Simulation Studies of Partial Demagnetization Process of Permanent Magnets in Electric Motors*, IEEE Transactions on Energy Conversion, vol. 36, no. 4, pp. 3137–3145 (2021), DOI: 10.1109/TEC.2021.3082903.

[8] Zawilak T., *Influence of rotor's cage resistance on demagnetization process in the line start permanent magnet synchronous motor*, Archives of Electrical Engineering, vol. 69, no. 2, pp. 249–258 (2020), DOI: 10.24425/aee.2020.133023.

[9] Lin D., Zhou P., Bracken E., *Generalized Algorithm to Deal with Temperature-Dependent Demagnetization Curves of Permanent Magnets for FEA*, IEEE Transactions on Magnetics, vol. 57, no. 11, pp. 1–6 (2021), DOI: 10.1109/TMAG.2021.3115431.

[10] Zhou P., Lin D., Xiao Y., Lambert N., Rahman M.A., *Temperature-Dependent Demagnetization Model of Permanent Magnets for Finite Element Analysis*, IEEE Transactions on Magnetics, vol. 48, no. 2, pp. 1031–1034 (2012), DOI: 10.1109/TMAG.2011.2172395.

[11] Kurihara K., Rahman M.A., *High-efficiency line-start interior permanent-magnet synchronous motors*, IEEE Transactions on Industry Applications, vol. 40, no. 3, pp. 789–796 (2004), DOI: 10.1109/TIA.2004.827476.

[12] Behbahanifard H., Sadoughi A., *Line Start Permanent Magnet Synchronous Motor Performance and Design; a Review*, Journal of World's Electrical Engineering and Technology, vol. 4, no. 2, pp. 58–66 (2015), https://www.semanticscholar.org/paper/Line-Start-Permanent-Magnet-Synchronous-Motor-and-a-Behbahanifard-Sadoughi/2502123ce179c551e0eba887a1bfe44e8d8420ba, accessed 21 April 2022.

[13] Ershad N.F., Mirsalim M., Aliabad A.D., *Line-start permanent magnet motors: proper design for pole-changing starting method*, IET Electric Power Applications, vol. 7, no. 6, pp. 470–476 (2013), DOI: 10.1049/iet-epa.2012.0059.

[14] Lu W., Zhao H., Liu S., *Demagnetization conditions comparison for line-start permanent magnet synchronous motors*, 17th International Conference on Electrical Machines and Systems (ICEMS), pp. 48–52 (2014), DOI: 10.1109/ICEMS.2014.7013449.

[15] Yingli L., Zhiqiang L., Mingji L., Lifang Z., *Analysis on fast reclosing of line start permanent magnet motor with time-stepping finite element method*, International Conference on Electrical Machines and Systems, pp. 3257–3261 (2008).

[16] Zhao W., Tian M., Wang X., Sun Y., *Analysis of the Synchronization Process and the Synchronization Capability for a Novel 6/8-Pole Changing LSPMSM*, IEEE Transactions on Magnetics, vol. 56, no. 2, pp. 1–6 (2020), DOI: 10.1109/TMAG.2019.2953286.

[17] Tian M., Wang X., Wang D., Zhao W., Li C., *A Novel Line-Start Permanent Magnet Synchronous Motor with 6/8 Pole Changing Stator Winding*, IEEE Transactions on Energy Conversion, vol. 33, no. 3, pp. 1164–1174 (2018), DOI: 10.1109/TEC.2018.2826550.